

Supplementary Information

Revealing the Stress Signature and Ion Origin of Metal Plating in Rechargeable Batteries

Table S1: Details of electrodes and substrate used for stress measurement

Hard Carbon Composite (single-sided, rolling pressed, from MTI Corporation, USA)

94.8 wt% HC (or active material)
2 wt% conductive Super-P
3.2 wt% polymer binder (1.2 wt% sodium carboxymethyl cellulose, CMC, and 2 wt% styrene–butadiene rubber, SBR)

<i>Current Collector (Al) Thickness</i>	<i>16 μm</i>
<i>Coating Thickness</i>	<i>88 μm</i>
<i>Total Coating Loading</i>	<i>8 mg cm^{-2}</i>
<i>HC Loading</i>	<i>7.58 mg cm^{-2}</i>

Graphite Composite (single-sided, rolling pressed, from MTI Corporation, USA)

93.2 wt% graphite powder (or active material)
2.5 wt% conductive Super-P
4.3 wt% polymeric binders (1.8 wt% CMC, and 2.5 wt% SBR)

<i>Current Collector (Cu) Thickness</i>	<i>9 μm</i>
<i>Coating Thickness</i>	<i>41 μm</i>
<i>Total Coating Loading</i>	<i>6.3 mg cm^{-2}</i>
<i>Graphite Loading</i>	<i>5.87 mg cm^{-2}</i>

Germanium Thin Film (DC sputter deposited)

<i>Current Collector (Cu) Thickness</i>	<i>200 nm</i>
<i>Film Thickness</i>	<i>155 nm</i>
<i>Approximate active material Loading</i>	<i>0.082 mg cm^{-2}</i>

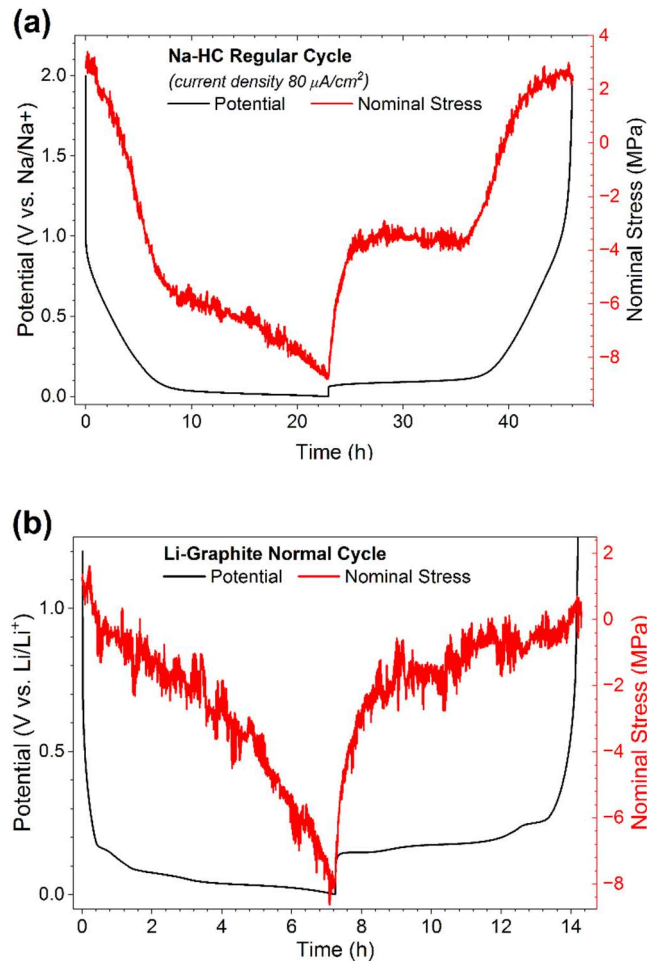
Fused Silica

<i>Young's modulus</i>	<i>71 GPa</i>
<i>Poisson's ratio</i>	<i>0.16</i>
<i>Thickness</i>	<i>500 μm</i>

*The area of the working electrode used in beaker cells was approximately 20 cm^2 .

S1. Potential and stress response of electrodes during regular (non-plating) cycles

The *in situ* stress evolution of the Hard Carbon (HC) composite electrode during the plating cycling is shown in Fig. S1a. The stress is tensile (~ 2 MPa) at the start of the experiment and becomes compressive during sodiation. This compressive stress increases nearly linearly in the sloping region of the potential profile: the stress value is -7 MPa at 0.1 V vs. Na/Na^+ . The stress continues to change during the plateau region albeit at a slower rate, reaching around -9 MPa at 0.005 V vs. Na/Na^+ . On desodiation, the stress immediately increases to -4 MPa and remains around this value for the duration of the voltage plateau (0.005 - 0.1 V vs. Na/Na^+). After this, because the Na storage mechanisms changes, the stress rises rapidly and eventually become tensile as the HC is fully desodiated at a potential of 2 V vs. Na/Na^+ .



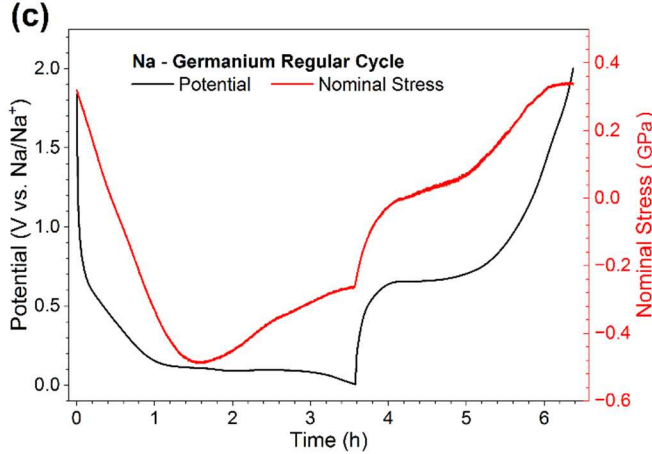


Fig. S1. Representative potential and stress evolution during regular (non-plating) galvanostatic cycles of (a) Na-hard carbon, (b) Li-Graphite, and (c) Na-Germanium system.

The *in situ* stress evolution of the graphite (Gr) composite electrode during the non-plating cycling is shown in Fig. S1b. The potential profile of graphite displays the well-known staging behavior, and consistent with prior reports [1] a compressive stress of up to -8 MPa is observed due to Li^+ intercalation between the graphite layers. On delithiation, the stress immediately increases to -4 MPa (~ 0.12 V vs. Li/Li^+) and then gradually increases, eventually becoming tensile as the graphite is fully delithiated (1.5 V vs. Li/Li^+).

Figure S1c presents the potential and stress response of an amorphous germanium (a-Ge) thin-film electrode cycled against Na foil. As the Na^+ ions alloy with Ge, the electrode expands generating compressive stress, up to approximately -0.5 GPa. The stress decrease to -0.27 GPa (at 5.25 h), which is due to the plastic deformation and change in the yield strength of the Na-Ge sample. On desodiation, the stress rapidly rises to around 0 GPa (0.65 V vs. Na/Na^+) and then continues to increase reaching a tensile value of around 0.35 GPa when the Ge is fully desodiated at a potential of 2 V vs. Na/Na^+ .

S2. Morphological (SEM and EDX) Study of Plating

To verify the interpretation of the onset and progression of sodium plating, a Na–HC half-cell was oversodiated to the appearance of the stress plateau (point B in Fig. 2b) and subsequently disassembled for SEM and EDX analyses. The pristine HC electrode served as a baseline, while the *sodiated* electrode (discharged to point X in Fig. 2b, but not below 0 V) was analyzed to quantify Na stored within the HC. The *plated* electrode (discharged beyond 0 V, point B) was used to examine the morphology and composition after plating. HC electrodes after stripping and desodiation was examined (charged to 2 V) to find the remaining Na within HC.

The SEM and EDX results for these electrodes are presented in Fig. 2, S2, and Table S2. The pristine HC (Fig. 2c) exhibited a negligible Na signal (~ 0.3 wt%), which likely originates from the sodium carboxymethyl cellulose (Na-CMC) binder and residual electrolyte. The carbon content (~ 99 wt%) reflects contributions from the hard carbon and small amounts from the binders (Na-CMC and SBR). In contrast, the *sodiated* (Fig. 2d) and *plated* electrodes (Fig. 2e) showed substantial sodium and oxygen content. The oxygen signal arises from partial oxidation of Na during specimen transfer from the glovebox to the SEM chamber. The *plated* Na layer covers the HC surface, consistent with the strong Na and O signals in the EDX spectra. Because EDX at a high acceleration voltage (20 kV, used in this study) probes both the surface and subsurface regions, the spectra reflect contributions from both metallic Na deposits and Na stored within the HC matrix.

Literature reports indicate that Na can form NaC_6 or NaC_8 intercalation compounds in HC during sodiation [2,3]. Theoretically, this corresponds to a Na content of ~ 19 – 24 wt% (based on the atomic masses of Na = 23 and C = 12). The 22.9 wt% Na detected in the *sodiated* specimen (at point X) therefore corresponds well to full intercalation of Na within the HC structure. In contrast, the *plated* specimen exhibited a significantly higher Na content (46.5 wt%), consistent with the coexistence of intercalated Na and metallic Na plated on the HC surface. The stripped and desodiated HC (Fig. 2f) showed a small amount of Na (~ 4.6 wt%), which could be from trapped sodium inside HC and dead Na metals.

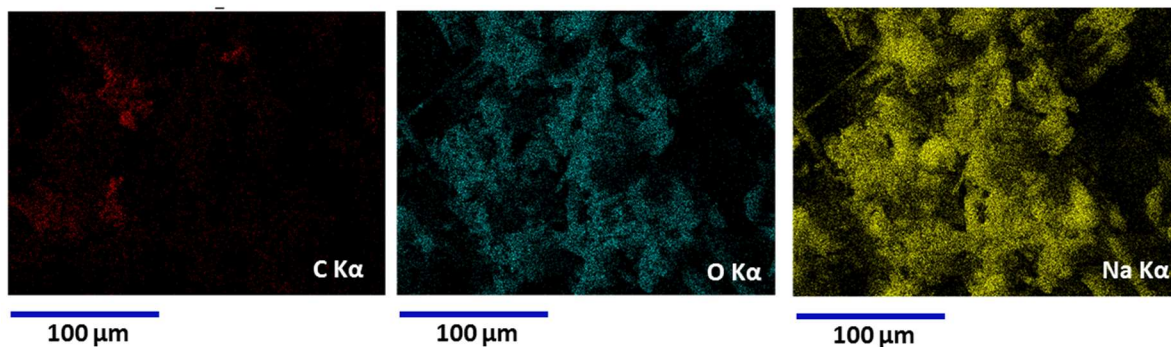


Fig. S2. EDX mapping showing elemental composition of hard carbon electrodes with plated sodium (from Fig. 2e).

Table S2. EDX analysis of pristine, sodiated, plated, and stripped-desodiated hard carbon (HC) electrodes

Sample	Carbon (wt%)	Sodium (wt%)	Oxygen (wt%)
Pristine HC	99.2	0.3	0
Sodiated HC (at point X in Fig. 2b, > 0 V)	43.5	22.9	33.0
Plated HC (after point B in Fig. 2b, < 0 V)	10.2	46.5	43.2
HC after stripping and de-sodiation (~100 h, Fig. 2a, 2 V)	86.4	4.6	6.1

S3. Stress response of sodiated HC electrode during OCP relaxation

Figure S3 shows the potential and stress responses of a sodiated hard carbon electrode held at open-circuit potential (OCP) immediately after complete sodiation (0.005 V vs. Na/Na⁺). The potential relaxed rapidly to a stable plateau, and the stress decreased correspondingly due to electrochemical–mechanical coupling. However, even after 16 h at OCP, the total stress

relaxation was only ~ 1 MPa, smaller than the pronounced stress reversal (3.29 MPa) observed at the onset of plating in Fig. 2.

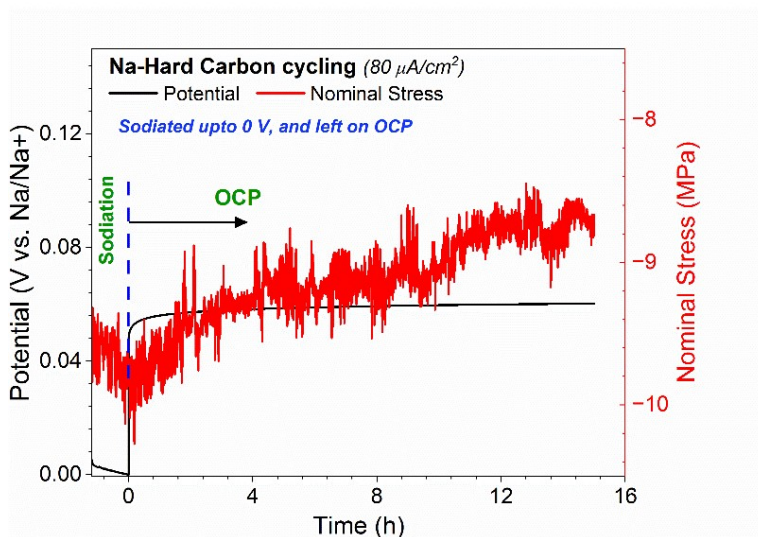


Fig. S3. Potential and stress evolution of a hard carbon electrode at open-circuit after full sodiation (0.005 V vs. Na/Na⁺).

S4. Stress measurement during Na-Al cycling

To consider the effect of metal nucleation, additional control experiment was carried out by plating Na on aluminum foil along with simultaneous stress measurement. A separate beaker cell was prepared with Na as the reference/counter electrode, while aluminum (Al) foil (bonded to Si-wafer) was used as the working electrode. The electrodes were separated by a glass fiber separator. As the Al is inert to Na, hence cycling Al against Na would not cause any Na intercalation, and any stress response observed would be purely due to the plating/stripping of Na on/from the Al. The Na/Al cell was cycled galvanostatically (at $\sim 20 \mu\text{A cm}^{-2}$) for 6 consecutive cycles (three cycles of 10 min each followed by three cycles of 20 min each) and the curvature or stress evolution during the process was simultaneously recorded.

As shown in Fig. S4a, the change in stress was almost negligible throughout the cycling of Na-Al cell. No significant change was observed during nucleation or the whole plating process (as shown in Fig. S4). Therefore, it can be concluded that other alternative mechanical origins (i.e., deposition of additional mass on surface, surface roughening during metal nucleation etc.) may have minimal effect on electrode stress. Hence, the stress reversal observed in this study can be attributed to the

volume change experienced by the working electrodes (HC, Ge) and were mainly due to the depletion of Na^+ ions.

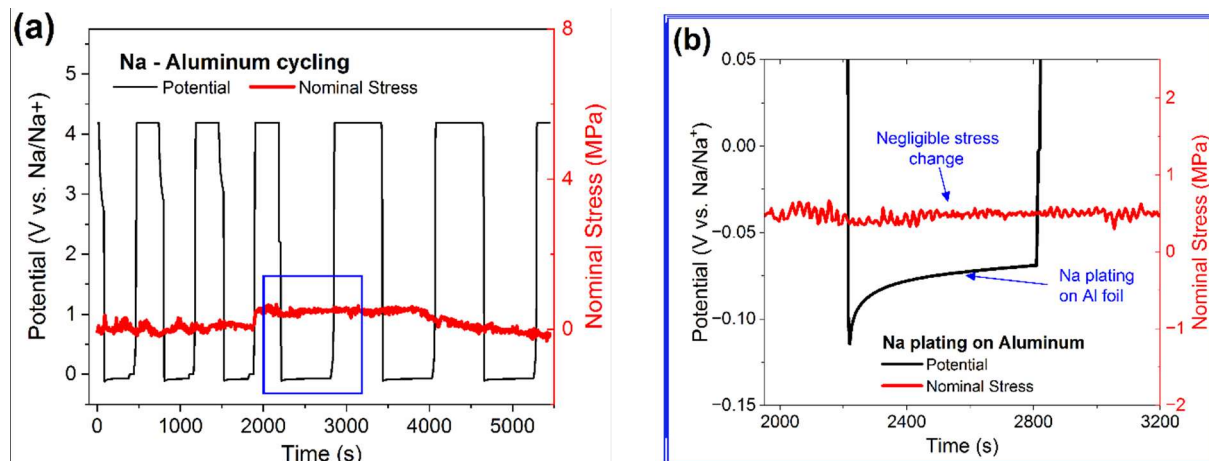


Fig. S4. Potential and stress evolution in a Na/Al cell during galvanostatic plating/stripping, (a) for six consecutive cycles, (b) inset (expanded view of one cycle).

References

- [1] V.A. Sethuraman, N. Van Winkle, D.P. Abraham, A.F. Bower, P.R. Guduru, Real-time stress measurements in lithium-ion battery negative-electrodes, *J. Power Sources*. 206 (2012) 334–342. <https://doi.org/10.1016/j.jpowsour.2012.01.036>.
- [2] N. Sun, Z. Guan, Y. Liu, Y. Cao, Q. Zhu, H. Liu, Z. Wang, P. Zhang, B. Xu, Extended “Adsorption–Insertion” Model: A New Insight into the Sodium Storage Mechanism of Hard Carbons, *Adv. Energy Mater.* 9 (2019) 1–14. <https://doi.org/10.1002/aenm.201901351>.
- [3] S. Qiu, L. Xiao, M.L. Sushko, K.S. Han, Y. Shao, M. Yan, X. Liang, L. Mai, J. Feng, Y. Cao, X. Ai, H. Yang, J. Liu, Manipulating Adsorption–Insertion Mechanisms in Nanostructured Carbon Materials for High-Efficiency Sodium Ion Storage, *Adv. Energy Mater.* 7 (2017) 1–11. <https://doi.org/10.1002/aenm.201700403>.